Hydrol. Earth Syst. Sci. Discuss., 12, 10109–10156, 2015
www.hydrol-earth-syst-sci-discuss.net/12/10109/2015/
doi:10.5194/hessd-12-10109-2015

Hydrology and Earth System Sciences
Open Access
Discussions

Impact of climate change on groundwater in a confined Mediterranean aquifer

Y. Caballero and B. Ladouche

BRGM, Water Environment and Ecotechnologies Division, 1039 rue de Pinville, 34000, Montpellier, France

Received: 23 July 2015 – Accepted: 10 August 2015 – Published: 2 October 2015

Correspondence to: Y. Caballero (y.caballero@brgm.fr)

Published by Copernicus Publications on behalf of the European Geosciences Union.

Abstract

This paper presents an inverse modeling method based on wavelet analysis, devoted to assessment of the impacts of climate change on the groundwater resources of a confined coastal multi-layer aquifer, located in the south of France (*Pyrénées-Orientales*). The hydraulic behavior of the aquifer is described based on the results of a model calibrated to simulate the groundwater dynamics observed on two representative piezometers. The relative contributions of the climate and pumping forcings to the piezometric variations are quantified. The results illustrate in quantitative terms the dominant influence of pumping on the temporal variations of the hydraulic head of the aquifer. Based on this specific behavior simulation, we show the moderate vulnerability of such confined aquifers to climate change. Some insights regarding pumping strategies for confined coastal aquifers that could contribute towards preserving their good status in future are also provided.

1 Introduction

Although groundwater resources are often critical for agricultural and drinking water uses, the impact of climate change on groundwater is less frequently analyzed than for surface water. Existing studies at the regional scale focus on changes of aquifer recharge using reservoir models employing precipitation and PET (Thomsen, 1990; Chen et al., 2002), aquifer storage (groundwater level) and drainage (spring flow) using water balance models (Döll, 2009; Rivard et al., 2014; Wada et al., 2014), three-dimensional finite difference groundwater models (Loaiciga et al., 2000; Allen et al., 2004; Serrat-Capdevila et al., 2007; van Roosmalen et al., 2007; Woldeamlak et al., 2007; Carneiro et al., 2010; Goderniaux et al., 2011; Habets et al., 2013; Castaño et al., 2013) or soil-vegetation-atmosphere transfer schemes (Bouraoui et al., 1999; Eckhardt and Ulbrich, 2003; Brouyère et al., 2004; Scibek and Allen, 2006; Caballero

et al., 2007; Crosbie et al., 2013; Portmann et al., 2013). For a complete review of climate change impacts on groundwater see Green et al. (2011).

Existing studies generally focus on unconfined aquifers because (1) they are generally shallow (2) they are often in hydraulic connection with surface water where river-groundwater interactions control the impact of recharge on both systems (Allen et al., 2004; Scibek and Allen, 2006). Nevertheless, confined aquifers are of great interest especially for water supply since they generally provide a water resource protected from anthropogenic pollution. The few existing assessments of climate change impact on confined aquifers are usually performed using complex hydrodynamic models (see Green et al., 2011 or more recent papers such as Ali et al., 2012). For such models, detailed descriptions of the geometry and the hydraulic properties of the different layers are required, for a correct estimation of the transient flow component of the recharge (Seiler et al., 2008), as the aquifer response to loading from surface recharge mainly depends on the change of pressure in the overlying confining units (Maliva et al., 2011).

For complex geological contexts such as those that can be found in the Mediterranean sedimentary rim (Duvail et al., 2005; Clauzon et al., 2015), the description of the layers geometry and hydraulic properties may be challenging enough to prevent the use of a hydrodynamic model. Alternative modeling methods able to simulate the climate change impact without a detailed description of the aquifer geometry are thus required.

This paper aims to present a modeling method based on wavelet analysis for the assessment of the climate change impact on a confined multi-layer aquifer affected by major pumping exploitation. Such a method allows fitting a numerical relation between climate, pumping and groundwater level variation, without explicitly taking into account the aquifer geometry and its hydraulic properties. It thus represents an interesting option to explore global (ie. both climate and economic – considering the link between future economic situation and the pumping withdrawals evolution to for the latter) change impacts on such kind of complex aquifers.

The following section describes the study area, the main hydrogeological characteristics of the confined aquifer studied, and the available data used for modeling. The third section presents a general description of the wavelet analysis and the way it has been used for the estimation of the pumped volumes and the groundwater level variation simulation. It also presents the climate scenarios used to force the model built. Results are presented and discussed in the fourth section, and main conclusions are summarized in the last section.

2 The Roussillon plain Plio–Quaternary (PQ) aquifer

The Roussillon basin is located along the southernmost part of the French Mediterranean coast, near the Spanish border. This 700 km^2 sedimentary basin is bordered by the foothills of the Pyrenean Mountains on the south and west, the Corbières karst region on the north and the Mediterranean Sea on the east (Fig. 1). It is embedded within a Miocene structured margin, the consequence of a marine regression following the Messinian salinity crisis (partial drying up of the Mediterranean Sea, approximately 6 My ago, Benson et al., 1991). The regression caused the excavation of deep canyons by fluvial erosion, which were then filled up with fluvial and marine sands, which now constitute various sedimentological units deposited according to the “Gilbert Delta” genetic model (Clauzon, 1990; Guennoc et al., 2000; Aunay et al., 2006). Two major aquifers, the Quaternary aquifer and the underlying continental and marine Pliocene aquifer, occupy these sediments.

The Quaternary one lies along the principal rivers (Agly, Têt and Tech) and the coastline, with thicknesses ranging from 10 m in the upper part of the valleys to more than 20 m in the coastal fringe (Aunay et al., 2006). It is mainly exploited by farmers, private individuals and campsite owners.

The Pliocene is divided into an upper system formed by prograding fluvial sands and a lower system of prograding marine sands and clays, separated by diachronous layers of lignite with plant remains alternating with marshy plastic-clays (Aunay et al.,

2006). Its depth increases towards the coastline, where its maximum thickness reaches 300 m (Duvail et al., 2005). Both sedimentological units constitute productive confined aquifers, with a transmissivity (and associated storage coefficient) ranging from $10^{-2}\,m^2\,s^{-1}$ ($4\times10^{-5}\,m^{-1}$) for the continental sands, to $10^{-3}\,m^2\,s^{-1}$ ($1\times10^{-5}\,m^{-1}$) for the marine sands (Chabart, 1996). These latter layers are not present everywhere, implying potential local connections between the upper and lower Pliocene aquifers (Aunay et al., 2006).

A network for monitoring groundwater status has enabled the compilation of a database of piezometric levels over periods in some cases exceeding 30 years for certain sites (Fig. 1).

The data acquired indicate that the groundwater flows from west to east in the Pliocene aquifers. The hydraulic gradient is low (about 1 to 4 ‰), and flow rates are probably less than ten meters per year (Chery, 1992). Fourty years ago the piezometric level of groundwater in the deep marine sands was artesian (Got, 1965; Aunay, 2007). Since then, major exploitation of the aquifers by drilling (essentially for drinking water supplies and agriculture) has caused a net decrease in the hydraulic loads, especially during the summer. In recent years and at certain sites, this decline has lowered the groundwater level below sea level during the summer months, when withdrawals are most intense.

The multilayer Plio–Quaternary Roussillon aquifer accounts for almost 80 % of the resources used for drinking water in the Département of Pyrénées Orientales. Withdrawals for this purpose have doubled in the past 30 years to 47 Mm^3 in 2007, including 29 Mm^3 from Pliocene formations (Terrasson et al., 2014). This increase in withdrawals is in line with the increase in the population within the study area which depend on this resource (+56 % in 30 years). However, a trend towards the stabilization of withdrawals for this purpose has been observed in recent years. Withdrawals from the Plio–Quaternary aquifer for uses other than drinking water supply are less well documented. They could be around 28 $Mm^3\,yr^{-1}$ (including 5 Mm^3 from the Pliocene) for agriculture, 4 Mm^3 from the Pliocene for industry, and 6 Mm^3 (including 1 Mm^3 in the Pliocene) from

private wells. Thus, the total annual withdrawals from the Plio–Quaternary aquifer for all uses would reach a total of 83 Mm^3, including 39 Mm^3 from the Pliocene (Terrasson et al., 2014). Accordingly, the importance of this aquifer for the Département's water resources quickly established a need to understand its functioning, so as to be able to manage the available resource in a sustainable manner.

A lot of work has been done to describe the structure and geometry of the Pliocene aquifer (Duvail et al., 2005; Chabart, 1996; Aunay, 2007); it emphasizes the strong spatial variation of the sedimentological units involved. The first difficulty faced when trying to deduce the hydrodynamic processes of the corresponding aquifers from their geological geometry is that there is a great lithological heterogeneity in the various sedimentological units described, e.g., continental sands and marine sands and clays. A consequence of this is that the hydrodynamic behavior of such units is also spatially variable. There are also connections between the units, which are not simple horizontal layers separated by units of low permeability but the distributary channels of a deltaic complex filled by sand. Moreover, many more than 500 boreholes have been drilled to exploit the available groundwater resource in the Roussillon basin, 35 % of which tap more than one sedimentological unit (Aunay, 2007). Thus pumping groundwater in a single borehole may have an impact on the hydraulic head of several sedimentological units. These major difficulties have so far prevented the construction of a 3-D gridded hydrodynamic model. Nonetheless, the monitoring network (Fig. 2) shows a rather coherent seasonal evolution of the groundwater levels at the scale of the whole aquifer system. Consequently, the evolution of one particular groundwater level time series of the piezometric network can roughly be considered representative of that of the whole aquifer system. Based on this fact, the data from two piezometers (10972X0137/PONT and 10908X0263/FIGUER), along those with the longer time series and located at contrasted distance of the sea shore (Fig. 1), have been analyzed to provide some insights about the dynamic of the whole aquifer system under present and future conditions.

3 Modeling method

3.1 General approach

Two piezometers The daily variations of the water levels observed in the piezometers at Perpignan (French Database Index 10908X0263/FIGUER) and Argelès (French Database Index 10972X0137/PONT) are shown in Fig. 3. The groundwater level's variation is affected by recharge from rainfall, and pumping for domestic, industrial or agricultural needs. The groundwater level time series show a seasonal cycle at the annual scale and a long term tendency to fall (Fig. 3). To analyze whether the pumping could explain this, the monthly variation of the total pumping volume of all the boreholes located on the Pliocene aquifer during the 1998–2007 period, is compared to both time series (Fig. 3). As regards confined groundwater, it is considered that all the pumping operations targeting the aquifer will impact the piezometric levels measured at any point on it (Sen, 1995, page 170). In this study, various areas containing pumping operations likely to affect the Perpignan and Argelès piezometers were defined, on the assumption that the water flows are mainly oriented from west to east (Fig. 1). On the pumping measurement series, the seasonal pumping (SP) can be distinguished from the permanent pumping (PP) (Fig. 3). The PP is estimated from the pump discharges during the winter months (October to March). The SP is calculated by subtracting the PP from the pump discharges (total pumping).

We assume that annual variations in the piezometry are linked to the SP, while the long-term trend is linked to the PP from drinking water withdrawals, which have continued to grow for nearly 30 years (Terrasson et al., 2014). To test and verify the effect of pumping on the piezometry we applied the techniques of signal processing, and in particular the use of continuous wavelets (wavelet analysis sub-section). Cross characterizations of pumping and piezometry for the period 1998–2008 were then used to estimate the volumes pumped over the period 1974–1997, for which the volumes pumped from Pliocene aquifers are poorly known (sub-section on estimation of pumped volumes).

Transfer models were then developed to model the observed piezometric variations (sub-section on Inverse modeling), taking as input components the computed withdrawals and the recharge (effective rainfall). Finally, these transfer models were used to simulate the impact of climate change on the Roussillon aquifer's water resources, and to facilitate its discussion.

3.2 Wavelet analysis

The variability and oscillations observed in the long-term hydrogeological time series in the monitored boreholes (Fig. 3) were studied using wavelet analysis. This analytic technique is now extensively used in geoscience for the visualization, identification and filtering of the main spectral components in time series (Labat, 2005, 2008, 2010; Lafrenière and Sharp, 2003; Maraun and Kurths, 2004; Yan and Jones, 2008). Choice of the appropriate wavelet depends on the nature of the signal and on the type of information to be extracted from it. We used the Continuous Wavelet Transform (CWT) to determine the dominant modes of variability and how those modes vary over time. The Paul wavelet method described in Torrence and Compo (1998), was chosen because, as reported by De Moortel et al. (2004), it allows a better time resolution, for any value of the wavelet parameter, than the Morlet wavelet.

Our wavelet analysis was aimed at the characterization of water-table variations in order to identify the energy associated with seasonal and long-term increases in pumping. The long-term trend was characterized by using the wavelet-filtered time series (Torrence and Compo, 1998). Calculations were performed using the Paul wavelet, taking into account the entire pass-band of the piezometric measurement series. The piezometric variables filtered by the Paul wavelet enable access to figures not influenced by the long-term trend linked to the increase in permanent pumping (Fig. 4). The difference between the wavelength-filtered record ($y1$) and the measured piezometric record ($y0$) enables the long-term variation of a trend ($y1 - y0$) to be characterized (Fig. 4). The situation at the beginning of the measurement series constitutes the reference value for each of the measurement series studied. The processing applied

shows that the long-term trend produced a water level drop of nearly 2 m for the Perpignan piezometer and 1.5 m for the Argelès piezometer, between the beginning and the end of their observation period. This reduction begins around 1982 in the case of Perpignan (Fig. 4b) and is expressed from the very beginning of the shorter Argelès measurement series (Fig. 4d).

The SP may be compared to a pseudo-periodic phenomenon. Characterization of the impact of this phenomenon on the piezometry can be addressed using the Scale–Averaged Wavelet Power (SAWP) (Torrence and Compo, 1998). The exercise amounts to determining the pass-band (bandwidth), which best represents the duration of this transient phenomenon. As a first step, the Fourier squared coherence (Torrence and Webster, 1999) was used to identify the time intervals (band) during which pumping and water level are covarying (Fig. 5). The pumping and water-level time series for the Perpignan and Argelès piezometers show significant wavelet-squared coherence in the 120 to 370 day band and low consistency outside these periods, i.e., not significant at the 95 % confidence level.

The SAWPs over the 120–370 day band for pumping and water level were calculated (Fig. 6a–d) for the Perpignan and Argelès piezometers. The variance in water level is well correlated with the changes in pumping, as shown in Fig. 6e and f. The normalized cross-wavelet spectrum exhibits maximum coherence during summer (August, Fig. 6e and f). The methodological approach developed here allows us to show that the piezometric decreases (drawdowns) observed during summer periods are mainly controlled by the seasonal increase in withdrawals (SP) from the Pliocene aquifer. The maximum SAWP corrected to the 95 % confidence level calculated for both piezometers is found in August (Fig. 5a and b). The energy of this Dirac function (called a comb function) estimated for the month of August, is assumed to be proportional to the cumulative SP discharge.

3.3 Estimation of pumped volumes

Over the period 1998–2007, the figures for the long-term trend ($y1 - y0$) are related to the variation of permanent pumping by power functions, best regression fit obtained with an origin passing by zero (Fig. 7). These functions enable reconstruction of the figures for the permanent pumping component for the period prior to 1998, for Perpignan and Argelès (Fig. 8). For the seasonal pumping, we employ the normalized cross-wavelet spectrum (Fig. 5e and f) to reconstruct it, based on the SAWP time series over the 120–371 day band for water level (Fig. 5a and b) for the period prior to 1998. The variation of seasonal pumping calculated and then reconstituted for the two piezometers during the period prior to 1998 is presented in Fig. 8. The functions established to reconstruct the permanent and seasonal pumping were then used as inputs for the transfer models applied to simulate the piezometric variations at Perpignan and Argelès (see “Inverse Modeling” section).

3.4 Inverse modeling

The hydrogeologic modeling was performed using transfer methods implemented with TEMPO software (Pinault, 2001). Calculation of the non-parametric impulse responses is achieved by inverse modeling with stress positivity. The term inverse modeling is here restricted to the parameter identification of convolution kernels used to simulate the output from the input. The calculation of impulse responses under stress allows the principle of conservation of water mass to be satisfied.

Computation of the impulse response uses regularization methods inspired by Tikonov and Arsenine (1976), Tikonov and Goncharsky (1987), and Dietrich and Chapman (1993), as described by Pinault et al. (2001a). The search for a solution by the regularization technique seeks to find the optimal solution for the transport equation (Eq. 1). Among all possible solutions, the approach of minimizing the norm of the transport equation allows selecting the solution with the smallest norm so as to smooth the non-parametric impulse response (Pinault et al., 2001a).

The inverse modeling approach appears to be well suited to characterizing the functioning of complex hydro-systems (Pinault et al., 2001a, b; Pinault et al., 2004, 2005; Pinault and Schomburgk, 2006; Dörfliger et al., 2009; Ladouche et al., 2014). In this study, the method used to simulate water-table variation in the PQ aquifer describes the fluctuations of the groundwater head by using components associated with recharge from rainfall, and seasonal and permanent pumping (Fig. 9), as described by the wavelet analysis.

The piezometric variation is described by the following convolution equation:

$$\Delta H(t) = \lambda \Gamma * R_{\text{eff}} + \lambda_1 \Gamma_1 * Q_{\text{SP}} + \lambda_2 \Gamma_2 * Q_{\text{PP}} + \lambda_3 \Gamma_3 * Q_{\text{Riv}} + \varepsilon \quad (1)$$

where $\Gamma, \Gamma_1, \Gamma_2$, and Γ_3 are the normalized non-parametric impulse responses (integrated area of the impulse response over its lag time equal to 1), Γ is the normalized impulse response of recharge from effective rainfall; Γ_1 is the normalized impulse response of seasonal pumping (SP); Γ_2 is the normalized impulse response of permanent pumping (PP); Γ_3 is the normalized impulse response of the river's contribution (Q_{Riv}), and ε represents the erratic contribution that is not described or explained by the model.

λ, λ_1, λ_2 and λ_3 are positive coefficients for expressing the conservation of water mass (the bar over the quantities indicate a mean value over the total calibration period):

$$\lambda \frac{\overline{R_{\text{eff}}}}{\overline{\Delta H}} + \lambda_1 \frac{\overline{Q_{\text{SP}}}}{\overline{\Delta H}} + \lambda_2 \frac{\overline{Q_{\text{PP}}}}{\overline{\Delta H}} + \lambda_3 \frac{\overline{Q_{\text{Riv}}}}{\overline{\Delta H}} = 1 \quad (2)$$

The term $\lambda_1 Q_{\text{SP}}$ allows us to describe the drawdown caused by the seasonal pumping (Q_{SP}). The term $\lambda_2 Q_{\text{PP}}$ describes the long term decreasing trend caused by the permanent pumping (Q_{PP}). The term $\lambda_3 Q_{\text{Riv}}$ allows us to describe the river contribution to recharge. The term λR_{eff} allows a description of the contribution from the effective rainfall.

The effective rainfall is calculated by:

$$R_{\text{eff}}(t) = R(t) - \Omega(t) \quad \text{if } R_{\Sigma}(t) \geq \Omega(t), \quad \text{otherwise } R_{\text{eff}}(t) = 0 \quad (3)$$

Where R is rainfall and Ω is a threshold function:

$$\Omega(t) = \text{Gr} * R(t) + \text{GTa} * \text{Ta}(t) + C \quad (4)$$

where $*$ is the discrete convolution product, t the time, C a constant, and Gr and GTa the impulse responses such that GTa > 0 and Gr < 0. These two impulse responses (Gr and GTa) are represented by trapezia (not shown). Details of the impulse response parameter calculation are presented in Pinault et al. (2001a).

The effective rainfall $R_{\text{eff}}(t)$ comprises two components: $R_{\text{eff}}(t) = R_{\text{s}}(t) + R_{\text{f}}(t)$, where $R_{\text{s}}(t)$ and $R_{\text{s}}(t)$ are the components of effective rainfall that respectively induce the slow and fast responses of the system. The fast component is assumed to be representative of the fast infiltration which occurs only after high-rainfall events. The component $R_{\text{f}}(t)$ is expressed according to $R_{\text{eff}}(t)$ by the Alpha function [$\alpha(t)$]:

$$R_{\text{f}}(t) = \alpha(t) \times R_{\text{eff}}(t) \quad (5)$$

where $\alpha(t)$ is the proportion of effective recharge (its values lies between 0 and 1). The Alpha function enables consideration of the non-linear switching behavior of the soil reservoir, which depends on the effective rainfall over the preceding days. The Alpha function is related to the effective recharge by the convolution product:

$$\alpha(t) = \Gamma_{\alpha,\text{Reff}} * R_{\text{eff}}(t) \quad (6)$$

where $*$ is the discrete convolution product, t the time, and $\Gamma_{\alpha,\text{Reff}}$ the impulse response of $\alpha(t)$ to effective rainfall $R_{\text{eff}}(t)$. The impulse responses are also represented by trapezia (not shown).

3.5 Climate scenarios

While early studies used simplified climate scenarios involving fixed ranges of precipitation or recharge against which to compare the groundwater response (Woldeamlak et al., 2007; Wilkinson and Cooper, 1993; Ferguson and Maxwell, 2010), an increasing number of studies now use climate scenarios derived from the outputs of climate models (Green et al., 2011). To build these climate scenarios, various methods of bias correction and downscaling are applied. These methods range from the simple but robust so-called perturbation method, based on the mean monthly differences between future and present measurements (Déqué, 2007), to more sophisticated methods (called statistical or dynamic) which mainly enable the distributions of future meteorological variables to be compared to present-day ones (Déqué, 2007; Boé et al., 2006; Fowler et al., 2007; Goderniaux et al., 2009, 2011).

In this study a set of five climate scenarios were constructed by using the perturbation method. This method consists of taking a meteorological data set representative of the present, and applying the mean monthly anomalies between future and present-day temperatures and precipitations simulated by the climate models (Déqué, 2007; Xu, 1999). Daily precipitation and potential evapotranspiration (PET) for the 1970–2006 period were extracted from the SAFRAN meteorological database (Vidal et al., 2010) available for the study zone on a regular 8 km × 8 km grid (Chaouche et al., 2010). Among the 21 climate-model outputs from the World Climate Research Program's (WCRP) Coupled Model Intercomparison Project Phase 3 (CMIP3) multi-model dataset (Meehl et al., 2007), which are available through the Program for Climate Model Diagnosis and Intercomparison (PCMDI), five climate models were selected over the French region. They were chosen as they were considered as able to capture both regional precipitation and temperature climatology for the Mediterranean region (Mariotti et al., 2008). These models are CNRM-CM3 (Salas y Melia et al., 2005), HadGEM1 (Johns et al., 2006), IPSL-CM4 (Hourdin et al., 2006), MPI-ECHAM5 (Roeckner et al., 2006; Jungclaus et al., 2006), and NCAR-CCSM3.0 (Collins et al., 2006). Atmospheric

temperature and precipitation (spatial resolution from 1 to 3.75°) were extracted for the French region (8° W to 10° E, 40° to 52° N) and for the 1980 2000 (reference), 2020–2040 (near-term), and 2040–2060 (medium-term) periods, and for the SRES-A1B scenario. This greenhouse-gas emission scenario is considered to be a compromise between a more optimistic scenario such as the SRES-B1 and a more pessimistic one such as the SRES-A2, although they differ only slightly for the period studied (Hourdin et al., 2006; Nakicenovic and Swart, 2000).

The mean monthly anomalies of temperature and precipitation calculated from the five climate models provide a description of the average climate change between the two future periods considered and the present, together with an illustration of the uncertainties associated with climate modeling. A multi-model average increase in temperature of between +1.0 and +1.8 °C is projected, depending on the season, for the near-term (2020–40) compared to the present. The projected increase is even greater for the medium term (204060), between +1.7 and 3.3 °C, with in addition a greater inter-seasonal variation compared to the near term. For precipitation, there is no clear signal for the near term (−10.9 to +10.5 % depending on the season), while a decrease (−21.9 to −2.1 %) is projected for the medium term. The large uncertainty associated with the calculated anomalies is higher for precipitation than for temperature, for summer than for winter, and for the medium term than for the near term.

More details about climate scenarios can be found in Caballero et al. (2008). While more sophisticated downscaling methods than the perturbation one (Quintana-Seguí et al., 2010) and new climate model simulations, like those carried out for the AR5 IPCC report, (Terray and Boé, 2013) have been performed on our study area, they have so far not produced sharply different results in terms of monthly average anomalies.

4 Results

4.1 Modeling of the piezometric levels at Argelès and Perpignan

The transfer model for the Argelés piezometer provides a satisfactory simulation of the 10 day sampling interval variations in the measured piezometry for the calibration period (Nash criterion = 0.82, Fig. 10a). These results were obtained without taking into account any recharge by the Tech River. The model was validated against the water levels measured for the 1990–1998 period (Fig. 12); it satisfactorily reproduces the seasonal pumping periods and the Nash criterion of 0.82 is considered acceptable.

The mean transit time (Tm) associated with the normalized impulse response is the mean value of the lag time (Pinault et al., 2005). The response of the aquifer to recharge by effective rainfall is highly inertial, since Tm is 220 days, for an impulse response length of 520 days (Fig. 10c). The relative contribution of a hydrological cycle's recharge (fast + slow component) results in piezometric variations of about 0.5 to 0.8 m (Fig. 10b). The relative contribution of SP to the variations in piezometry is about −0.8 m over a hydrological cycle (Fig. 10b). The maximum response of the aquifer to seasonal pumping (SP) is detected during the month of August (Fig. 6f). It occurs 75 days after the start of pumping (Fig. 10d). The increase in PP over the period 1991–2007 is expressed by a decrease in the piezometry of about −0.6 m over the 17 years considered.

For the Perpignan site, the transfer model allows reproduction of the measured piezometric variations only if a water supply from the Têt River is considered. The transfer model enables a satisfactory reproduction of the variation in the groundwater level measured at the Perpignan piezometer (Nash criterion = 0.85, Fig. 11a). The model was validated with the water levels observed for the 1976–1994 period (Fig. 11a) which were satisfactorily reproduced (Nash criterion = 0.66). The flow rate of the Têt River upstream of the Roussillon plain is sustained in spring and summer by the release of water from the Vinca dam, which introduces a phase shift in the river's flow regime with respect to its natural regime. The contribution of recharge by precipitation thus differs

both temporally and quantitatively from the releases at the dam on the Têt (the recharge causes an increase in the piezometric level of a maximum of 0.5 m and is expressed mainly in winter, whereas the Têt's contribution causes a rise in the level of between 0.3 and 0.8 m, generally expressed in the summer – Fig. 11b). The response of the aquifer to recharge by effective rainfall appears less inertial than that characterized at Argelès (maximum and mean response time 60 and 89 days respectively – Fig. 11c). The aquifer's response to recharge by releases from the dam reaches a maximum after 70–80 days (Fig. 11c). This maximum response is detected in late July, which is consistent with the fact that the dam releases occur generally in April of each year.

Seasonal pumping (SP) causes piezometric variations of between −1.8 and −3 m over a hydrological cycle (Fig. 11b). The aquifer's maximum response to seasonal pumping (SP) occurs 75 days after the start of pumping (Fig. 11d); this maximum response is detected in late June (Fig. 6e) vs. late July for Argelès (Fig. 11b). For Perpignan, recharge by the Têt River, which is at a maximum during July, masks the effect of seasonal pumping (SP), which should reach its maximum in late July.

The increase in PP over the period 1974–2007 is expressed by a decrease in the piezometry of about −0.9 m over the 33 year period studied. Table 1 summarizes the characteristics of the models applied to reproduce the piezometric variations observed in the Argelès and Perpignan piezometers. The greater inertia observed at Argelès is illustrated by smaller piezometric variations (cf. Figs. 11a and 12, lower panel), a greater impulse-response length (520 days for Argelès and 300 days for Perpignan) and a markedly longer average transit time (Tm: 220 days for Argelès vs. 89 days for Perpignan). It also shows the spatial heterogeneity of the hydraulic behavior of the sandy Pliocene formations.

Near Perpignan, we note that the Pliocene aquifer responds to releases from the Têt dam more slowly than to recharge (τ3: 70–80 d vs. τ: 60 d in Table 1). This is probably connected to the fact that the water released at the dams is mostly directed to irrigated areas, sometimes located more than 20 km downstream, via canals which may or may not be leakproof. These canals enable the irrigation of tree and truck-farming crops

on the plain. The water not consumed by irrigated crops contributes to recharging the Quaternary alluvial water tables, formerly exploited to provide drinking water. Alluvial groundwater can contribute locally to the underlying Pliocene formations (Aunay, 2007).

Finally, the effect of permanent pumping (PP) on the piezometry is comparable for the two sites and is expressed by a decrease of about 30 to 40 cm per decade. To assess the quality of the simulation performed, sensitivity analyses were carried out on variations in the forcings (recharge and pumping) used in the transfer model developed for Argelès (Fig. 12).

The behavior of the model was accordingly evaluated for a period of 11 years in the absence of pumping [a], and then for a reduction in precipitations of about 50 % [b] and 90 % [c] with respect to the test period, under pumping conditions (for SP and PP) identical to those of 2006. A test with pumping shut down shows that the simulated piezometric levels quickly rise up again and then stabilize at an elevation of about 9.5 m NGF. This result strengthens confidence in the quality of the model since (1) It simulates a piezometric level in the absence of pumping that is higher than the figures observed at the beginning of the available measurement series (about 9 m NGF at a period when pumping was weaker than at any other point in the time series), and (2) the simulated level stabilizes at a figure close to the piezometric level measured during the installation of the meter, in 1984 (9.7 m a.s.l. – Infoterre Argelès, 2013).

The test of major decrease in rainfall shows the expected disappearance of the effect of recharge and a stabilization of the water level, which no longer fluctuates except under the effect of seasonal pumping (SP), producing variations of about 1 m. The model thus reproduces the confined nature of the aquifer.

4.2 Impacts of climate change

The impact of climate change on the simulated piezometric levels was assessed using the model constructed for the Argelès piezometer. This analysis could not be performed for the Perpignan piezometer because this would require an explicit simulation of flows in the Têt River and the management of the Vinca dam in the context of a future climate.

The results obtained for the reference scenario [1980–2000 period] were compared with the results of the scenarios for the near [2020–2040] and medium [2040–2060] terms from the five climate models (CNRM; HADC; IPSL; MPIM; NCAR) and the MULTI model (multi model average). The simulations were performed with and without pumping. The pumping scenario considered (PS and PP) is identical to that for the year 2008, i.e., the pumpings are identical from one cycle to another over the 20 years considered in the analysis, for current and future periods.

The variations of the interannual monthly means of simulated effective rainfall over the reference period (1980–2000), the near (2020–2040) and the medium (2040–2060) terms are compared on Fig. 13. The multi-model mean and the envelope curves limited by the minimum and maximum values calculated from the monthly means of effective rainfall in all scenarios, which represent their dispersion, are shown. In the near term, effective winter rainfalls would be comparable to those in the reference period, although they should be lower in the spring (−20 to −50 % in the multi-model mean). However, high uncertainty is associated with these variations because they fall within the scenarios' tolerance interval. In autumn, the effective rainfall should also be lower (from −20 to −30 % in the multi-model mean), compared to those in the reference period, with greater certainty than in the spring, given the smaller dispersion of the scenarios in October and November. In the medium term, the downward signal grows stronger, both in intensity and in certainty, as future variations fall out of the scenarios' tolerance interval. Thus a sharp drop in effective rainfall may be observed in the spring (from −20 to −90 % in the multi-model mean), as well as in the fall and early winter (−30 to −60 %) as compared to the reference period. Only the effective rainfalls of November and January appear unchanged.

The variation of the interannual monthly means of the simulated piezometric levels for the reference scenario (1980–2000) and future climate scenarios (2020–2040 and 2040–2060), with and without pumping, are compared on Fig. 14. In the near term (2020–2040), the piezometric levels in the absence of pumping appear comparable to those in the reference scenario (monthly interannual range of variability expressed

by the standard deviation overlaps those falling between the minimum and maximum figures obtained for all scenarios – Fig. 14 upper panel, left). Under permanent pumping only (SC1) or both permanent and seasonal (SC2), the piezometric level would fall slightly in all months of the year. However, the scenarios' tolerance interval includes this situation, indicating that the observed decrease is probably not significant.

In the medium term (2040–2060), piezometric levels in the absence of pumping would fall significantly in every season (the scenarios' tolerance interval is located outside the current monthly interannual range of variability – Fig. 14 upper panel, right). We see here that the projected drop in recharge in the autumn and spring (Fig. 13) produces a decrease in the piezometric level year-round (a result related to the system's inertia). Taking into account the pumping (SC1 or SC2, Fig. 14, middle and lower panels, right), does not change the order of magnitude of the projected decline.

5 Discussion

The modeling methods based on wavelet analysis presented in this paper have enabled us to simulate the behavior of a confined aquifer with a highly complex hydrogeology, in the vicinity of two observation piezometers. They also allowed us develop a descriptive outline of the principal processes involved. Thus, while the behavior of this aquifer as observed at the various existing monitoring stations seems fairly homogeneous (seasonal fluctuation of groundwater levels characterized by a downward trend over the last 30 years), the modeling performed has identified a number of processes at work, depending on the areas considered.

Firstly, the Argelès area exhibits a behavior that seems more inertial than the one at Perpignan. This is expressed (Table 1) by a longer duration and mean transit time of the normalized impulse response, and a smaller relative contribution of the SP to water-level changes for Argelès. Nonetheless, the sensitivity of its changes in water-level to effective rainfall is slightly greater than that at Perpignan, and its lag time for maximum response of the normalized impulse response is shorter. This means that

the transfer of hydraulic head linked to recharge into the aquifer is faster for the Argelès area than for Perpignan. The more inertial character of Argelès expresses the lower transmissivity of the aquifer in this area as compared to Perpignan, which is consistent with the orders of magnitude estimated by interpretation of the pumping tests available for the aquifer (Aunay, 2007). The greater sensitivity of the piezometric level at Argeles could be explained by a smaller storage coefficient, but this parameter of the aquifer is poorly known (Aunay, 2007).

Finally, the faster transfer of pressure (30 days for Argelès vs. 60 at Perpignan) could be explained by a higher diffusivity (ratio of transmissivity to storage coefficient), reflecting that the aquifer is more confined in the Argelès sector than in the Perpignan sector.

However, other factors may also explain the difference in behavior between the two areas. The thicker Quaternary formations which overlie the Pliocene ones in the Perpignan area could have a buffering effect on the infiltration of effective rainfall (Fig. 1). The formations of the Corbières karstic system, which have circulations at depths of more than 100 m, recharge the Pliocene aquifer at depth (Aunay, 2007), probably with a time-lag after rainfall. Lastly, the presence of a large network of canals, used for irrigation and fed from the dam on the Têt, may also cause a delay in the infiltration of effective rainfall. To distinguish the effects of these various factors on the behavior of the groundwater, it would be necessary to explicitly incorporate into the modeling not only the Quaternary and karstic formations but also the layout of the canals.

Secondly, the analysis highlights the overall preponderant influence, at the annual scale, of the withdrawals by SP and PP as compared to the recharge, which explains the continued decline in water levels observed throughout the measurement series. The modeling shows that the trend component corresponding to PP affects both sites in the same way (decrease of about 0.3 m decade^{-1}). The relative contribution of SP to water level changes is higher for Perpignan than for Argelès (Table 1), while the lower transmissivities in this area should lead to larger drawdowns.

This is probably related to the fact that, for Argelès, the contribution of the Tech river was not explicitly taken into account because it is synchronous with the contribution from precipitation. However, this contribution is probably included in the two seasonal components used in the model (recharge and SP). In this case, it leads to an overestimation of the recharge component and/or an underestimation of the SP component (hence its smaller contribution to water level changes as compared to that seen at Perpignan),although it is impossible to quantify them. Since the contribution of the Têt river is explicitly taken into account in modeling the piezometric level at Perpignan (via the releases from the Vinca dam), the quantification of the SP component is probably more realistic than at Argelès.

Figure 12 (case a) shows that if pumping stops, the simulated water level rises abruptly back up, reaching an equilibrium level in less than one hydrological cycle. This is related to the mean transit time of the impulse response to effective rainfall employed in the model, whose duration is less than one year (Table 1). Similarly, if we consider a zero recharge (Fig. 12b and c), the simulated piezometric level remains at an equilibrium level and does not fall over time, in spite of the pumping. The model thus expresses the highly confined nature of the aquifer in the Argelès area, where variations in the piezometric level are controlled by rapid changes of pressure within the aquifer rather than by a flow dynamic known to be slow (flow rates of less than10 m yr^{-1}, obtained from tritium and carbon-14 dating by Chery, 1992). However, although the functioning of the model in a no-recharge situation may be viewed as realistic, transient variations of the piezometric level are mainly controlled by the permanent pumping (the model was constructed on the assumption that the long-term trend is fully explained by the signal of increase in the PPs). This explains why the simulated piezometric level remains stable on Fig. 12b and c, instead of gradually falling under the effect of pumping, in the absence of recharge. Now, a rising trend in the temperatures of the study area was noted between 1971 and 2000 (Chaouche et al., 2010). This increase may have caused a reduction in the effective rainfall over the period 1970–2008. In this regard, a portion of the downward trend in water levels could also be related to long-

term climate variability. This is the major limitation of the modeling approach adopted, and which we cannot escape when dealing with confined aquifers subjected to major exploitation by pumping.

The tests presented in Fig. 12 show that the equilibrium state of the water levels in the Argelés area is controlled by PPs. If permanent pumping on the aquifer were doubled, it is probable that the model would simulate a fall in the piezometric level until it reached a new steady state. From a hydrodynamic perspective it can therefore be considered that this aquifer would be capable of supporting a larger pumping operation. The aquifer thus appears to be relatively invulnerable to climate change. This idea is backed up by the projections in Fig. 13, which show that in the medium term the simulated piezometric level for Argelès would be affected by a decrease of no more than about 0.5 m. This decrease is less than that caused by the current exploitation of the aquifer (which produces a decrease of more than 1.5 m, taking PP and SP together). It would therefore appear possible to offset the declining recharge projected in the climate scenarios by a well thought-out exploitation of the aquifer, which could probably be achieved with improved water-use efficiency and water-demand management (Green et al., 2011). The relationship between the volume pumped by the PP and the drop in the water level (Fig. 7) indicates that over the near and medium term we could maintain the current piezometric level by retaining the current permanent pumping of about 7 million m^3 (vs. about 8 million currently) for Perpignan and 2 million m^3 (vs. some 2.2 million at present) for Argelès.

Nevertheless, the vulnerability of this coastal aquifer to saline intrusion problems may still be exacerbated by the effect of CC. If we extrapolate the simulated medium-term fall in piezometric level at Argelès (of about 50 cm) to the station at Barcarès (French database index 0912X0112/BAR3), located on the beach at the mouth of the Agly river, its piezometric level would fall to about 2 m below sea level under summer conditions. The great sensitivity of the water level to seasonal pumping identified by the modeling (Figs. 10 and 11) could then be used to limit this fall by reducing coastal withdrawals during the summer. This reduction could be offset by pumping in wintertime or alter-

natively by an increase in withdrawals near the massifs. This is all the more plausible since simulation tests have shown similar modeling results whether we consider the pumping boreholes in the areas outlined in Fig. 1 or those throughout the whole study area (not shown). This means that given constant withdrawals across the region, pumping carried out sufficiently far from a given point will not impact its piezometric behavior. This feature could therefore be used to limit the decrease imposed by climate change on coastal piezometers.

The work presented in this article constitutes a modeling exercise; the representativeness of its results for the aquifer as a whole may be questioned. The first limit that can be identified resides in the fact that the two piezometers at Argelès and Perpignan are installed in formations that are not exactly the same throughout the sedimentary package that makes up the aquifer. This is expressed by their very different impulse response characteristics for recharge (the formations tapped at Perpignan exhibiting a lesser inertia than the ones at Argelès). Despite this, the confined nature of the aquifer is expressed by a great similarity among the piezometric behaviors observed in all the piezometers, particularly in coastal areas, insofar as they respond primarily to pressure transfers.

It is therefore probable that the magnitude of the impact of the diminished recharge projected for Argelès (around 0.5 m) can be extrapolated to the entire aquifer. The second limit deserving of attention lies in the fact that the modeling performed does not permit a rigorous exploration of the future vulnerability of the aquifer to saline intrusions. Indeed, the decreases in water level simulated for the near and medium term are likely to intensify this vulnerability, especially along the coast.

To explicitly incorporate this issue in the analysis, it will be necessary to simulate the variation of the quality of the water in the aquifer, and in particular its salinity.

6 Conclusions

This article shows how wavelet analysis techniques can be utilized as an alternative to hydrodynamic models for confined aquifers, whose geological complexity prevent a detailed description of the geometry and the hydraulic properties of the saturated and overlying units. Using these techniques, the variation of groundwater levels in two piezometers installed in a confined, heavily exploited aquifer of a Mediterranean coastal zone has been simulated. They were implemented in order to take into account the impact of pumping on drawdown of the water table and, by doing so, to simulate the unimpacted piezometric measurement series.

The proposed approach enabled us to identify and rank the factors that affect the seasonal fluctuations of the water table, and to improve our conceptual model of the aquifer.

On the one hand, the predominant influence of pumping, as the main factor controlling drawdown of the water table, has thereby been highlighted. For a complete understanding of the piezometric variation, it appeared also necessary to take into account the contributions of surface waters in the catchment areas bordering the aquifer (streams and karstic aquifers). Lastly, differences in hydrodynamic behavior between the two areas studied were described in a qualitative manner. On the other hand, it appeared that the wavelet analysis is unable to distinguish between the influences of components whose temporal dynamics are too similar, such as recharge by rainfall and by streams reacting to that rainfall.

The assembled model was then used to study the impact of climate change (five scenarios) on the aquifer's water resources. The reduction in future precipitation predicted by the scenarios is expressed in a moderate decrease in effective rainfall and in the piezometric level of the water table (50 cm); however, this decrease becomes significant in the medium term (2050), in spite of the high uncertainty associated with rainfall predictions. This relatively low vulnerability is explained by the confined nature of this aquifer, whose balance is controlled by pumping. This impact could quite easily

be limited by a change in the pumping strategy for the aquifer, which might equally well consist of taking less water each year, or a better distribution of withdrawals between the summer and winter seasons, or between withdrawals at the coast and near the mountains. Nevertheless, the relative invulnerability to climate change of confined aquifers of the type studied in this article must be placed in context, inasmuch as the modeling carried out does not take into account the problem of saline intrusions. It appears likely that the decline in water level projected under future climates might encourage the infiltration of sea water. The rise in sea level correlated with the predicted future warming trend reinforces the necessity of incorporating it into the analysis. In this regard, only hydrodynamic modeling based on a description of the geometry of the aquifers and their relationship with the sea will enable us to study this issue.

Acknowledgements. Y. Caballero and B. Ladouche designed the simulation strategy and the results analysis, B. Ladouche developed the model code and performed the simulations. Y. Caballero and B. Ladouche prepared the manuscript. This study was supported by the National Research Agency (Agence Nationale pour la Recherche – ANR) through its VMC 2006 program (VULCAIN Project, Contract-ANR-06-VULN-008-01) and the French Geological Survey (Bureau de Recherches Géologiques et Minières – BRGM). The authors would like to thank their VULCAIN partners for their contributions. We are also grateful to the modeling groups, the Program for Climate Model Diagnosis and Intercomparison (PCMDI) and the WCRP's Working Group on Coupled Modeling (WGCM) for their roles in making available the WCRP CMIP3 multi-model dataset. Support of this dataset is provided by the Office of Science, U.S. Department of Energy. The authors thank J.C. Marechal for assisting in organizing this paper.

References

Ali, R., McFarlane, D., Varma, S., Dawes, W., Emelyanova, I., Hodgson and Charles, G., S.: Potential climate change impacts on groundwater resources of south-western Australia, J. Hydrol., 475, 456–472, doi:10.1016/j.jhydrol.2012.04.043, 2012.

Allen, D. M., Mackie, D. C., and Wei, M.: Groundwater and climate change: a sensitivity analysis for the Grand Forks aquifer, southern British Columbia, Canada, Hydrogeol. J., 13, 270–290, 2004.

Aunay, B.: Apport de la stratigraphie séquentielle à la gestion et à la modélisation des ressources en eau des aquifères côtiers, available at: https://tel.archives-ouvertes.fr/tel-00275467, (last access: 25 September 2015), 2007.

Aunay, B., Duvail, C., Giordana, G., Dörfligher, N., Le Strat, P., Montginoul, M., and Pistre, S.: A pluridisciplinary methodology for integrated management of a coastal aquifer, Geological, hydrogeological and economic studies of the Roussillon aquifer (Pyrénées-Orientales, France), Life and Environment, 56, 275–285, 2006.

Benson, R. H., Rakic-El Bied, K., and Bonaduce, G.: An important current reversal (influx) in the Rifian Corridor (Morocco) at the Tortonian-Messinian boundary: the end of the Tethys Ocean, Paleoceanography, 6, 164–192, 1991.

Boé, J., Terray, L., Habets, F., and Martin, E.: A simple statistical-dynamical downscaling scheme based on weather types and conditional resampling, J. Geophys. Res., 111, D23106, doi:10.1029/2005JD006889, 2006.

Bouraoui, F., Vachaud, G., Li, L. Z. X., Le Treut, H., and Chen, T.: Evaluation of the impact of climate changes on water storage and groundwater recharge at the watershed scale, Clim. Dynam., 15, 153–161, doi:10.1007/s003820050274, 1999.

Brouyère, S., Carabin, G., and Dassargues, A.: Climate change impacts on groundwater resources: modelled deficits in a chalky aquifer, Geer basin, Belgium, Hydrogeol. J., 12, 123–134, 2004.

Caballero, Y., Voirin-Morel, S., Habets, F., Noilhan, J., LeMoigne, P., Lehenaff, A., and Boone, A.: Hydrological sensitivity of the Adour-Garonne river basin to climate change, Water Resour. Res., 43, W07448, doi:10.1029/2005WR004192, 2007.

Caballero, Y., Chaouche, K., Neppel, L., Salas y Melia, D., Martin, E., Terrasson, I., Chazot, S., Citeau, J. M., Maton, L., Rinaudo, J. D., Fleury, P., Ladouche, B., Dörfliger, N., and Pinault, J. L.: Vulnerability of Mediterranean hydrosystems to climate changes and human activities: the project,VULCAIN, Montpellier, 1er au 4 septembre 2008, 20, available at: http://www.iwra.org/congress/2008/index.php?page=proceedings&abstract_id=62, (last access: 17 July 2014), 2008.

Carneiro, J. F., Boughriba, M., Correia, A., Zarhloule, Y., Rimi, A., and El Houadi, B.: Evaluation of climate change effects in a coastal aquifer in Morocco using a density-dependent numer-

ical model, Environmental Earth Sciences, 61, 241–252, doi:10.1007/s12665-009-0339-3, 2010.
Castaño, S., Sanz, D., and Gómez-Alday, J. J.: Sensitivity of a groundwater flow model to both climatic variations and management scenarios in a semi-arid region of SE Spain, Water Resour. Manag., 27, 2089–2101, doi:10.1007/s11269-013-0277-4, 2013.
Chabart, M.: La recharge de l'aquifère multicouche du Roussillon et les conséquences d'un éventuel changement climatique sur la gestion des ressources en eau (Pyrénées Orientales), Doctorat en Hydrogéologie, Université de Paris VI, 299 pp., 1996.
Chaouche, K., Neppel, L., Dieulin, C., Pujol, N., Ladouche, B., Martin, E., Salas y Melia, D., and Caballero, Y.: Analyses of precipitation, temperature and evapotranspiration in a French Mediterranean region in the context of climate change, CR Geosci., 342, 234–243, doi:10.1016/j.crte.2010.02.001, 2010.
Chen, Z., Grasby, S. E., and Osadez, K. G.: Predicting average annual groundwater levels from climatic variables: an empirical model, J. Hydrol., 260, 102–117, 2002.
Chery, L.: Interpretation des resultats des analyses isotopiques des eaux du multicouche du Roussillon, n° BRGM/RR-36094-FR, 1–39, available at: http://www.brgm.fr/publication/pubDetailRapportSP.jsp?id=RSP-BRGM/RR-36094-FR, (last access: 17 July 2014), 1992.
Clauzon, G.: Restitution de l'évolution géodynamique néogène du bassin du Roussillon et de l'unité adjacente des Corbières d'après les données écostratigraphiques et paléogéographiques, Paléobiologie Continentale, Montpellier, 17, 125–155, 1990.
Clauzon, G., Le Strat, P., Duvail, C., Do Couto, D., Suc, J., Molliex, S., Bache, F., Besson, D., Lindsay, E. H., Opdyke, N. D., Rubino, J., Popescu, S., Haq, B. U., and Gorini, C.: The Roussillon Basin (S. France): a case-study to distinguish local and regional events between 6 and 3 Ma, Mar. Petrol. Geol., in press, doi:10.1016/j.marpetgeo.2015.03.012, 2015.
Collins, W. D., Bitz, C. M., Blackmon, M. L., Bonan, G. B., Bretherton, C. S., Carton, J. A., Chang, P. D., S. C., Hack, J. J., Henderson, T. B., Kiehl, J. T., Large, W. G., McKenna, D. S., Santer, B. D., and Smith, R. D.: The Community Climate System Model Version 3 (CCSM3), J. Climate, 19, 2122–2143, doi:10.1175/JCLI3761.1, 2006.
Crosbie, R. S., Scanlon, B. R., Mpelasoka, F. S., Reedy, R. C., Gates, J. B., and Zhang, L.: Potential climate change effects on groundwater recharge in the High Plains Aquifer, USA, Water Resour. Res., 49, 3936–3951, doi:10.1002/wrcr.20292, 2013.

De Moortel, I., Munday, S. A., and Hood, A. W.: Wavelet analysis: the effect of varying basic wavelet parameters, Sol. Phys., 222, 203–228, doi:10.1023/B:SOLA.0000043578.01201.2d, 2004.
Déqué, M.: Frequency of precipitation and temperature extremes over France in an anthropogenic scenario: model results and statistical correction according to observed values, Global Planet. Change, 57, 16–26, doi:10.1016/j.gloplacha.2006.11.030, 2007.
Dietrich, C. R. and Chapman, T. G.: Unit graph estimation and stabilization using quadratic programming and difference norms, Water Resour. Res., 29, 2629–2635, 1993.
Döll, P.: Vulnerability to the impact of climate change on renewable groundwater resources: a global-scale assessment, Environ. Res. Lett., 4, 035006, doi:10.1088/1748-9326/4/3/035006, 2009.
Dörfliger, N., Fleury, P., and Ladouche, B.: Inverse modeling approach to allogenic karst system characterization, Ground Water, 47, 414–426, doi:10.1111/j.1745-6584.2008.00517.x, 2009.
Duvail, C., Gorini, C., Lofi, J., Lestrat, P., Clauzon, G., and Dosreis, A.: Correlation between onshore and offshore Pliocene–Quaternary systems tracts below the Roussillon Basin (eastern Pyrenees, France), Mar. Petrol. Geol., 22, 747–756, doi:10.1016/j.marpetgeo.2005.03.009, 2005.
Eckhardt, K. and Ulbrich, U.: Potential impacts of climate change on groundwater recharge and streamflow in a central European low mountain range, J. Hydrol., 284, 244–252, 2003.
Ferguson, I. M. and Maxwell, R. M.: Role of groundwater in watershed response and land surface feedbacks under climate change, Water Resour. Res., 46, W00F02, doi:10.1029/2009WR008616, 2010.
Fowler, H. J., Kilsby, C. G., and Stunell, J.: Modelling the impacts of projected future climate change on water resources in north-west England, Hydrol. Earth Syst. Sci., 11, 1115–1126, doi:10.5194/hess-11-1115-2007, 2007.
Goderniaux, P., Brouyère, S., Fowler, H. J., Blenkinsop, S., Therrien, R., Orban, P., and Dassargues, A.: Large scale surface–subsurface hydrological model to assess climate change impacts on groundwater reserves, J. Hydrol., 373, 122–138, doi:10.1016/j.jhydrol.2009.04.017, 2009.
Goderniaux, P., Brouyère, S., Blenkinsop, S., Burton, A., Fowler, H. J., Orban, P., and Dassargues, A.: Modeling climate change impacts on groundwater resources

using transient stochastic climatic scenarios, Water Resour. Res., 47, W12516, doi:10.1029/2010WR010082, 2011.
Got, H.: Contribution à l'étude géologique et hydrogéologique de la région de Feuilla-Fitou (Corbières) et de la Salanque, http://www.sudoc.fr/071401032, (last access: 25 September 2015), 158 pp., 1965.
Green, T. R., Taniguchi, M., Kooi, H., Gurdak, J. J., Allen, D. M., Hiscock, K. M., Treidel, H., and Aureli, A.: Beneath the surface of global change: impacts of climate change on groundwater, J. Hydrol., 405, 532–560, doi:10.1016/j.jhydrol.2011.05.002, 2011.
Guennoc, P., Gorini, C., and Mauffret, A.: Histoire géologique du golfe du Lion et cartographie du rift oligo-aquitanien et de la surface messinienne, Géol France, 3, 67–97, 2000.
Habets, F., Boé, J., Déqué, M., Ducharne, A., Gascoin, S., Hachour, A., Martin, E., Pagé, C., Sauquet, E., Terray, L., Thiéry, D., Oudin, L., and Viennot, P.: Impact of climate change on the hydrogeology of two basins in northern France, Climatic Change, 121, 771–785, doi:10.1007/s10584-013-0934-x, 2013.
Hourdin, F., Musat, I., Bony, S., Braconnot, P., Codron, F., Dufresne, J., Fairhead, L., Filiberti, M., Friedlingstein, P., Grandpeix, J., Krinner, G., LeVan, P., Li, Z., and Lott, F.: The LMDZ4 general circulation model: climate performance and sensitivity to parametrized physics with emphasis on tropical convection, Clim. Dynam., 27, 787–813, doi:10.1007/s00382-006-0158-0, 2006.
Infoterre Argelès: available at: http://ficheinfoterre.brgm.fr/InfoterreFiche/ficheBss.action?id=10972X0137/PONT, (last access: 17 July 2014), 2013.
Johns, T. C., Durman, C. F., Banks, H. T., Roberts, M. J., McLaren, A. J., Ridley, J. K., Senior, C. A., Williams, K. D., Jones, A., Rickard, G. J., Cusack, S., Ingram, W. J., Crucifix, M., Sexton, D. M. H., Joshi, M. M., Dong, B., Spencer, H., Hill, R. S. R., Gregory, J. M., Keen, A. B., Pardaens, A. K., Lowe, J. A., Bodas-Salcedo, A., Stark, S., and Searl, Y.: The New Hadley Centre Climate Model (HadGEM1): evaluation of coupled simulations, J. Climate, 19, 1327–1353, doi:10.1175/JCLI3712.1, 2006.
Jungclaus, J. H., Keenlyside, N., Botzet, M., Haak, H., Luo, J., Latif, M., Marotzke, J., Mikolajewicz, U., and Roeckner, E.: Ocean circulation and tropical variability in the coupled model ECHAM5/MPI-OM, J. Climate, 19, 3952–3972, 2006.
Labat, D.: Recent advances in wavelet analyses: Part 1 – a review of concepts, J. Hydrol., 314, 289–311, 2005.
Labat, D.: Wavelet analysis of the annual discharge records of the world's largest rivers, Adv. Water Resour., 31, 109–117, doi:10.1016/j.advwatres.2007.07.004, 2008.

Labat, D.: Cross wavelet analyses of continental freshwater discharge and selected climates indices, J. Hydrol., 385, 269–278, doi:10.1016/j.jhydrol.2010.02.029, 2010.
Ladouche, B., Marechal, J.-C., and Dorfliger, N.: Semi-distributed lumped model of a karst system under active management, J. Hydrol., 509, 215–230, doi:10.1016/j.jhydrol.2013.11.017, 2014.
Lafrenière, M. and Sharp, M.: Wavelet analysis of inter-annual variability in the runoff regimes of glacial and nival stream catchments, Bow Lake, Alberta, Hydrol. Process., 17, 1093–1118, doi:10.1002/hyp.1187, 2003.
Loaiciga, H. A., Maidment, D. R., and Valdes, J. B.: Climate-change impacts in a regional karst aquifer, Texas, USA, J. Hydrol., 227, 173–194, 2000.
Maliva, R. G., Coulibaly, K., Guo, W., and Missimer, T. M.: Confined aquifer loading: implications for groundwater management, Ground Water, 49, 1–3, doi:10.1111/j.1745-6584.2010.00776.x, 2010.
Maraun, D. and Kurths, J.: Cross wavelet analysis: significance testing and pitfalls, Nonlin. Processes Geophys., 11, 505–514, doi:10.5194/npg-11-505-2004, 2004.
Mariotti, A., Zeng, N., Yoon, J., Artale, V., Navarra, A., Alpert, P., and Li, L. Z. X.: Mediterranean water cycle changes: transition to drier 21st century conditions in observations and CMIP3 simulations, Environ. Res. Lett., 3, 044001, 8 pp., 2008.
Meehl, G. A., Covey, C., Delworth, T., Latif, M., McAvaney, B., Mitchell, J. F. B., Stouffer, R. J., and Taylor, K. E.: The WCRP CMIP3 multimodel dataset: a new era in climate change research, B. Am. Meteorol. Soc., 88, 1383, doi:10.1175/BAMS-88-9-1383, 2007.
Nakicenovic, N. and Swart, R.: Emissions Scenarios. A Special Report of Working Group II of the Intergovernmental Panel on Climate Change, Publisher: Cambridge University Press, Cambridge, UK, ISBN: 0521800811, 570 pp., 2000.
Pinault, J. L.: Manuel utilisateur de TEMPO: Logiciel de traitement et de modélisation des séries temporelles en hydrogéologie et en hydrogéochimie, Rep. BRGM/RP-51459 -FR, 233 pp., Project Modhydro, Bur. de Rech. Geol. et. Miner., Orleans, France, 2001.
Pinault, J. L. and Schomburgk, S.: Inverse modeling for characterizing surface water/groundwater exchanges, Water Resour. Res., 42, W08414, doi:10.1029/2005WR004587, 2006.
Pinault, J. L., Pauwels, H., and Cann, C.: Inverse modeling of the hydrological and the hydrochemical behavior of hydrosystems: application to nitrate transport and denitrification, Water Resour. Res., 37, 2179–2190, doi:10.1029/2001WR900017, 2001a.

Pinault, J. L., Plagnes, V., Aquilina, L., and Bakalowicz, M.: Inverse modeling of the hydrological and the hydrochemical behavior of hydrosystems: characterization of Karst System Functioning, Water Resour. Res., 37, 2191, doi:10.1029/2001WR900018, 2001b.

Pinault, J. L., Dörfliger, N., Ladouche, B., and Bakalowicz, M.: Characterizing a coastal karst aquifer using an inverse modeling approach: the saline springs of Thau, southern France, Water Resour. Res., 40, W08501, doi:10.1029/2003WR002553, 2004.

Pinault, J. L., Amraoui, N., and Golaz, C.: Groundwater-induced flooding in macropore dominated hydrological system in the context of climate changes, Water Resour. Res., 41, W05001, doi:10.1029/2004WR003169, 2005.

Portmann, F. T., Döll, P., Eisner, S., and Fl, M.: Impact of climate change on renewable groundwater resources: assessing the benefits of avoided greenhouse gas emissions using selected CMIP5 climate projections, Environ. Res. Lett., 8, 024023-, doi:10.1088/1748-9326/8/2/024023, 2013.

Quintana-Seguí, P., Ribes, A., Martin, E., Habets, F., and Boé, J.: Comparison of three downscaling methods in simulating the impact of climate change on the hydrology of Mediterranean basins, J. Hydrol., 383, 111–124, doi:10.1016/j.jhydrol.2009.09.050, 2010.

Rivard, C., Paniconi, C., Vigneault, H., and Chaumont, D.: A watershed-scale study of climate change impacts on groundwater recharge (Annapolis Valley, Nova Scotia, Canada), Hydrolog. Sci. J., 59, 1437–1456, doi:10.1080/02626667.2014.887203, 2014.

Roeckner, E., Brokopf, R., Esch, M., Giorgetta, M., Hagemann, S., Kornblueh, L., Manzini, E., Schlese, U., and Schulzweida, U.: Sensitivity of simulated climate to horizontal and vertical resolution in the ECHAM5 atmosphere model, J. Climate, 19, 3771–3791, 2006.

Salas-Mélia, D., Chauvin, F., Déqué, M., Douville, H., Gueremy, J. F., Marquet, P., Planton, S., Royer, J. F., and Tyteca, S.: Description and validation of the CNRM-CM3 global coupled model, CNRM working note 103, available at: http://www.cnrm.meteo.fr/scenario2004/references_eng.html, (last access: 17 July 2014), 2005.

Scibek, J. and Allen, D. M.: Modeled impacts of predicted climate change on recharge and groundwater levels, Water Resour. Res., 42 doi:10.1029/2005WR004742, 2006, 2006.

Seiler, K. P., Gu, W. Z., and Stichler, W.: Transient response of groundwater systems to climate changes, Geol. Soc. Spec. Publ., 288, 111–119, doi:10.1144/SP288.9, 2008.

Sen, Z.: Applied Hydrogeology for Scientists and Engineers, 464 pp., CRC Press, Boca Raton, Lewis Publishers, USA, ISBN 9781566700917, 1995.

Serrat-Capdevila, A., Valdes, J. B., González-Pérez, J., Baird, K., Mata, L. J., and Maddock, T.: Modeling climate change impacts – and uncertainty – on the hydrology of a riparian system: the San Pedro Basin (Arizona/Sonora), J. Hydrol., 347, 48–66, doi:10.1016/j.jhydrol.2007.08.028, 2007.

Terrasson, I., Chazot, S., Maton, L., Rinaudo, J., and Caballero, Y.: Les Pyrénées Orientales face aux changements globaux: comparaison des effets des changements climatique et anthropique sur les besoins en eau, La Houille Blanche, n° 3, p. 53–63, 2014.

Terray, L. and Boé, J.: Quantifying 21st-century France climate change and related uncertainties, CR Geosci., 345, 136–149, doi:10.1016/j.crte.2013.02.003, 2013.

Thomsen, R.: Effect of climate variability and change in groundwater in Europe, Nord. Hydrol., 21, 185–194, 1990.

Tikhonov, A. and Arsenine, V.: Méthodes de Résolution de Problèmes mal Posés, MIR, Moscow, 1976.

Tikhonov, A. N. and Goncharsky, A. V. (Eds.): Ill-Posed Problems in the Natural Sciences, MIR, Moscow, 1987.

Torrence, C. and Compo, G. P.: A practical guide for wavelet analysis, B. Am. Meteorol. Soc., 79, 1, 61–78, 1998.

Torrence, C. and Webster, P. J.: Interdecadal changes in the ENSO–monsoon system, J. Climate, 12, 2679–2690, doi:10.1175/1520-0442(1999)012<2679:ICITEM>2.0.CO;2, 1999.

Van Roosmalen, L., Christensen, B. S. B., and Sonnenborg, T. O.: Regional differences in climate change impacts on groundwater and stream discharge in Denmark, Vadose Zone J., 6, 554, doi:10.2136/vzj2006.0093, 2007.

Vidal, J. P., Martin, E., Franchistéguy, L., Baillon, M., and Soubeyroux, J. M.: A 50 year high-resolution atmospheric reanalysis over France with the Safran system, Int. J. Climatol., 30, 1627–1644, doi:10.1002/joc.2003, 2010.

Wada, Y. and Bierkens, M. F. P.: Sustainability of global water use: past reconstruction and future projections, Environ. Res. Lett., 9, 104003, doi:10.1088/1748-9326/9/10/104003, 2014.

Wilkinson, W. B. and Cooper, D. M.: The response of idealized aquifer/river systems to climate change/Reponse de systemes aquifere-riviere schematiques aux modifications climatiques, Hydrolog. Sci. J., 38, 379–390, doi:10.1080/026266693099492688, 1993.

Woldeamlak, S. T., Batelaan, O., and De Smedt, F.: Effects of climate change on the groundwater system in the Grote-Nete catchment, Belgium, Hydrogeol. J., 15, 891–901, 2007.

Xu, C.-Y.: From GCMs to river flow: a review of downscaling methods and hydrologic modelling approaches, Prog. Phys. Geog., 23, 229–249, 1999.
Yan, Z. and Jones, P. D.: Detecting inhomogeneity in daily climate series using wavelet analysis, Adv. Atmos. Sci., 25, 157–163, doi:10.1007/s00376-008-0157-7, 2008

Table 1. Main characteristics of the modeling for the Argelès and Perpignan piezometers. τ is the normalized impulse response of the recharge from effective rainfall; $\tau 1$ is the normalized impulse response of the SP; $\tau 2$ is the normalized impulse response of the PP; $\tau 3$ is the normalized impulse response of the Têt river contribution.

Parameter	Argelès	Perpignan
Nash index for the calibration period	0.82	0.85
Nash index for the validation period	0.71	0.66
Relative contribution of effective recharge to water level changes	From +0.5 to +0.8 m	< 0.5 m
Length of the normalized impulse response of the effective rainfall (τ)	520 days	300 days
Mean transit time (Tm) of the normalized impulse response of (τ)	220 days	89 days
Lag for the maximum response of the normalized impulse response (τ)	30 days	60 days
Relative contribution of the seasonal pumping (SP) to water level changes	−1 m	From −1.8 m to 3 m
Date for the maximum contribution of the seasonal pumping (calculated from $\tau 1$)	Mid-Aug	End of Jun
Relative contribution of permanent pumping (PP) to water level changes	−0.6 m over 17 years	−0.9 m over 33 years
Relative contribution of the river to water level changes	–	From +0.2 to 0.8 m
Lag for the maximum response of the normalized impulse response ($\tau 3$)	–	70–80 days
Date for the maximum contribution of the river (calculated from $\tau 3$)	–	End of Jul

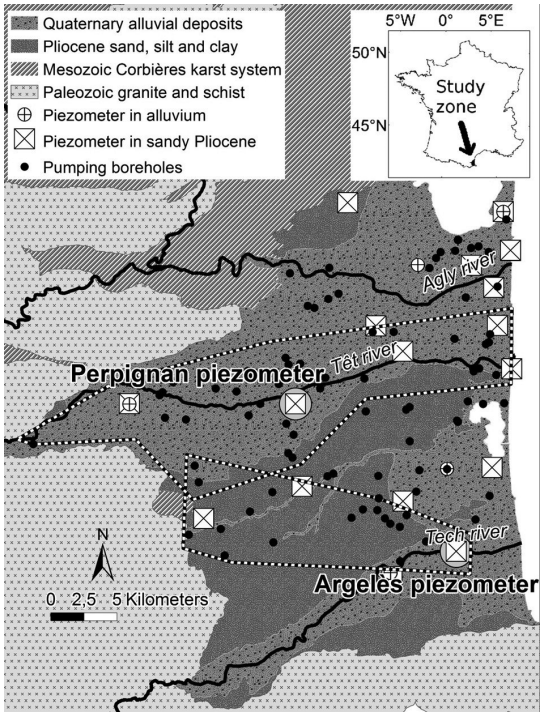

Figure 1. Geological context and piezometric network locations for monitoring the Roussillon Plio–Quaternary aquifer. Two specific piezometers (Perpignan and Argelès) are highlighted, over which modeling has been performed. Dashed outlines show the boreholes that were taken into account for each piezometer.

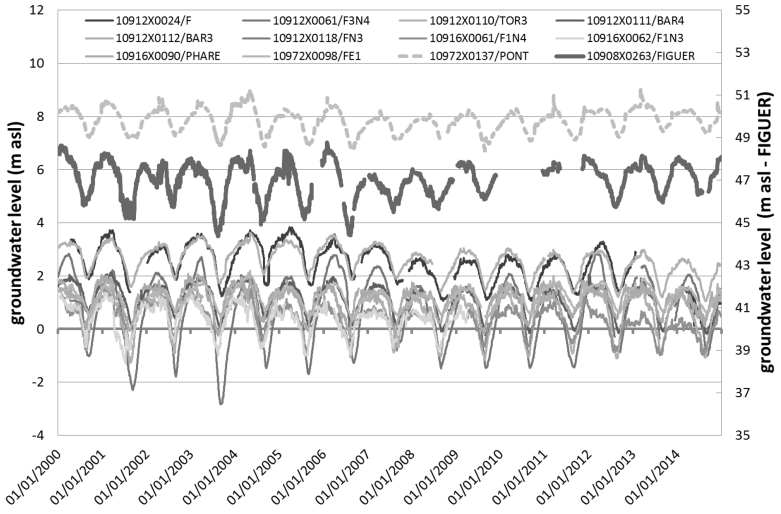

Figure 2. Groundwater level time series recorded over the last 15 years with the piezometer network of the Pliocene aquifer.

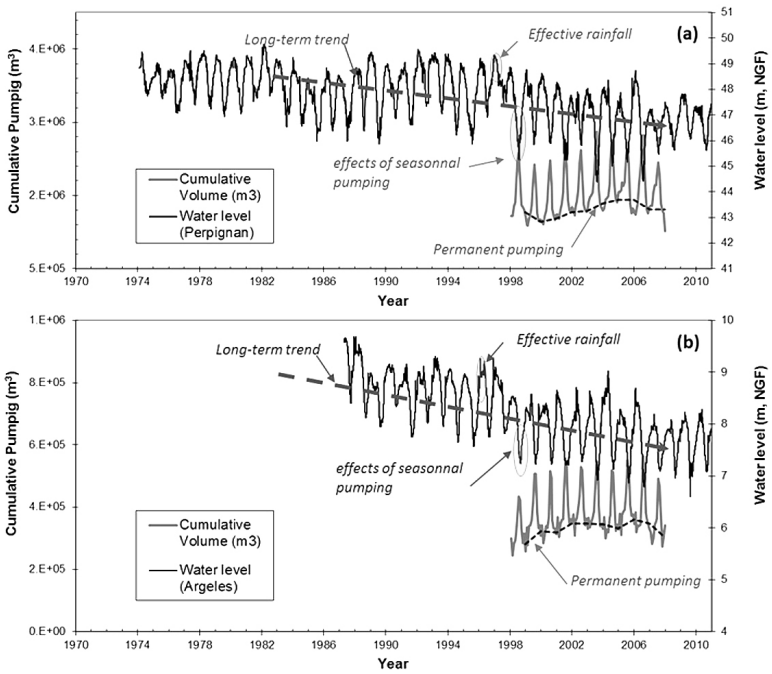

Figure 3. Daily piezometric data (m a.s.l.) at Perpignan **(a)** and Argelès **(b)** (see Fig. 1 for location) showing the long-term depletion trend, the effect of recharge by net rainfall, and the effect of summer water withdrawals. Pumping cumulated at the yearly time scale for the 1998–2007 period is also shown. The thin dashed line represents the permanent pumping equivalent of pumping during the winter period (October to March).

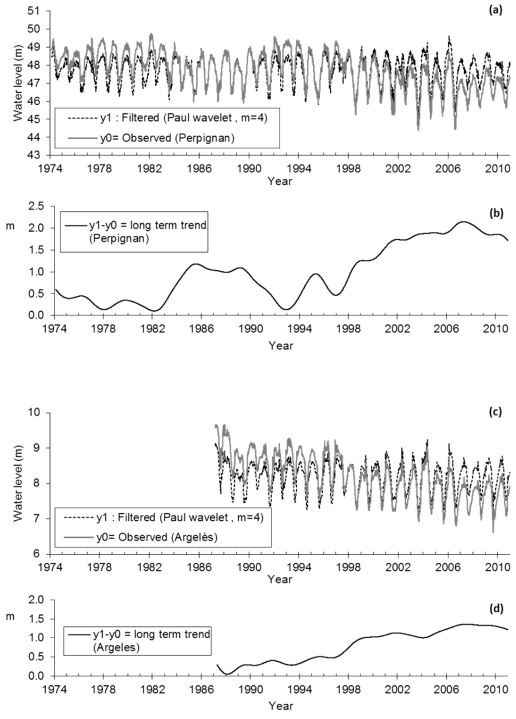

Figure 4. Wavelet-filtered time series of water levels (Perpignan and Argelès) computed with the Paul wavelet.

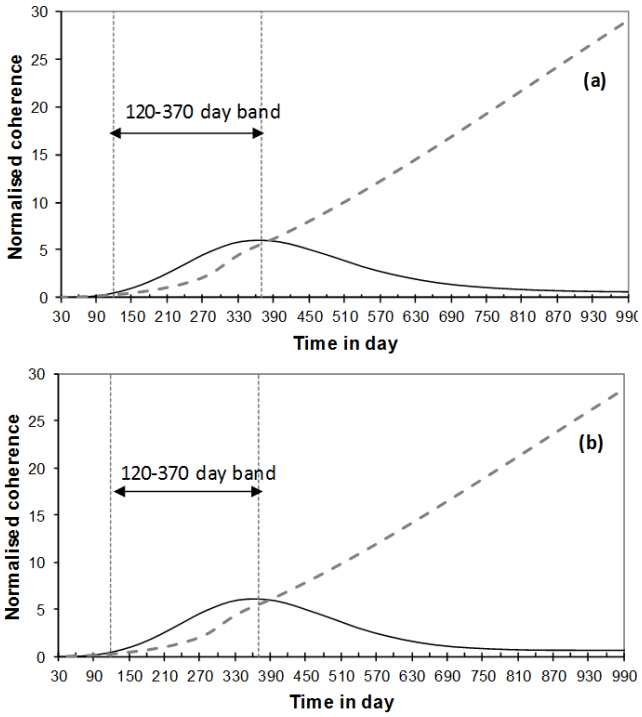

Figure 5. Fourier squared coherence calculated with Paul wavelet ($m = 4$) between pumping data (input) and water level (output) for the Perpignan piezometer **(a)** and Argelès piezometer **(b)** The dashed line is the 95 % confidence level.

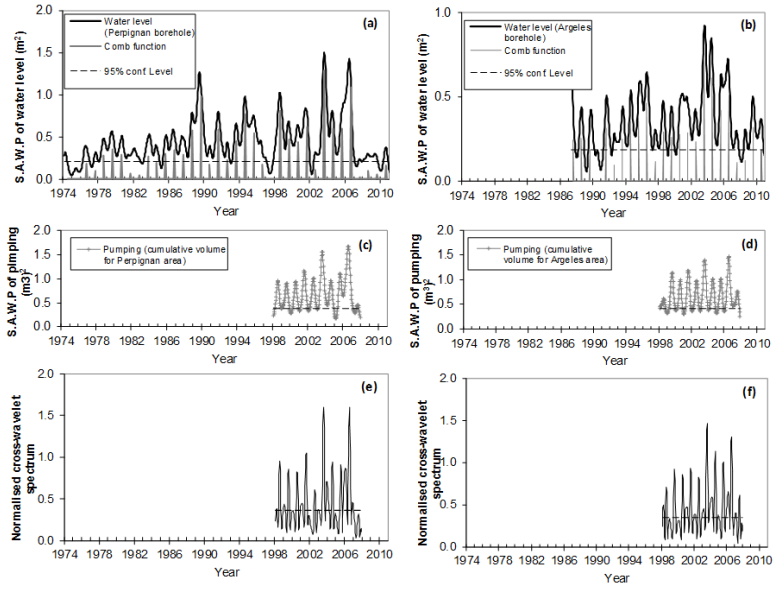

Figure 6. (a, b) Scale–Averaged Wavelet Power (SAWP) over the 120–371 day band for water levels measured in the Perpignan **(a)** and Argelès **(b)** piezometers using the Paul wavelet ($m = 4$). The dashed line is the 95 % confidence level. The thin solid line is the SAWP corrected to the 95 % confidence level, calculated for the month of August. This function is called the "comb function". **(c, d)**: SAWP over the 120–371 day band for pumping in the Perpignan area **(c)** and Argelès area **(d)** using the Paul wavelet ($m = 4$). The dashed line is the 95 % confidence level. **(e, f)**: cross SAWP over the 120–371 day band with pumping data (input) and water level (output) calculated with the Paul wavelet ($m = 4$) for Perpignan **(e)** and Argelès **(f)**. The dashed line is the 95 % confidence level.

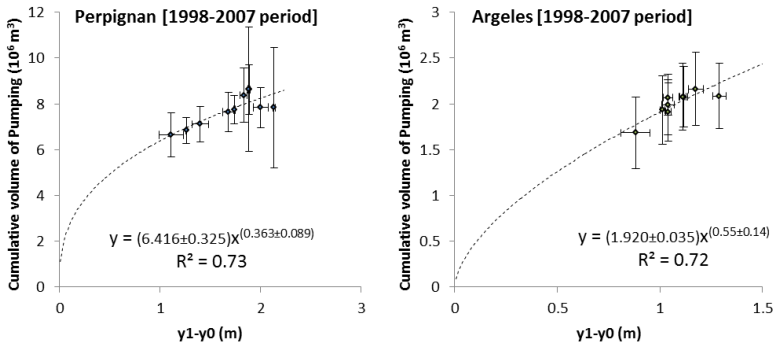

Figure 7. Changes in the volume of PP (1998–2007 period) based on the long-term trend.

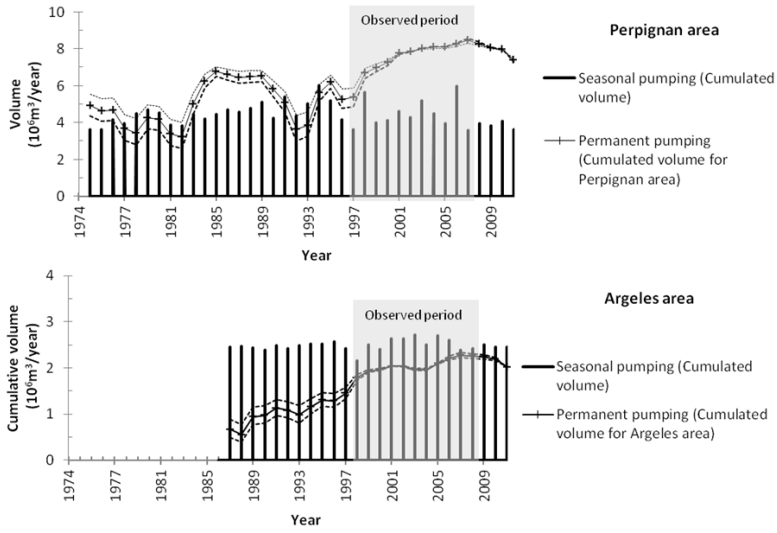

Figure 8. Variation of pumped volumes observed between 1998 and 2007 and reconstituted volumes for the preceding period. The permanent pumping was estimated from the long-term trend deduced from the Wavelet-filtered time series. The seasonal pumping volume (comb function) was estimated from the maximum SAWP (corrected to the 95 % confidence level) calculated for the month of August.

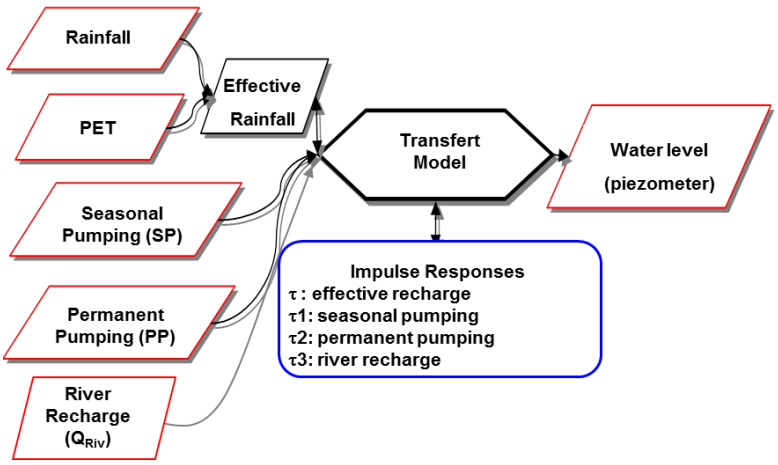

Figure 9. Architecture of the model used to simulate the water levels in the Perpignan and Argelès piezometers located on the PQ aquifer.

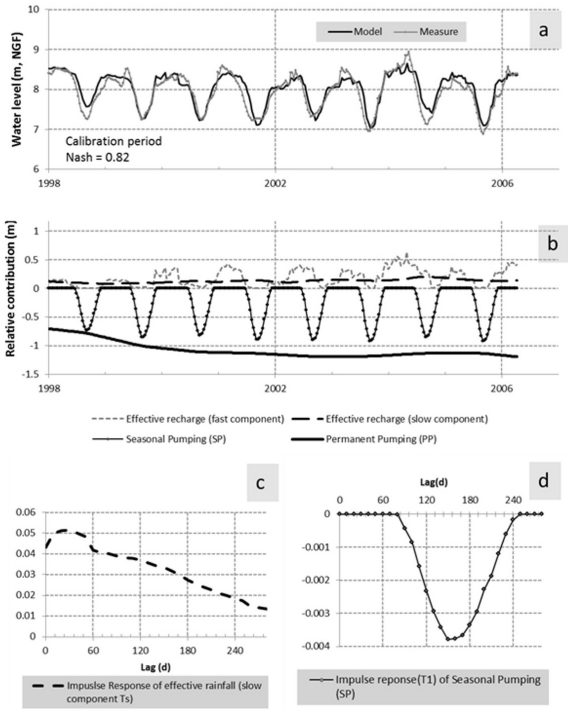

Figure 10. Inverse modeling of Pliocene confined aquifer (Argelès Piezometer) with a 10 day step. The measured and simulated piezometry is shown **(a)** as well as the relative contribution of the components **(b)**, the impulse response of recharge **(c)** and of the SP **(d)**.

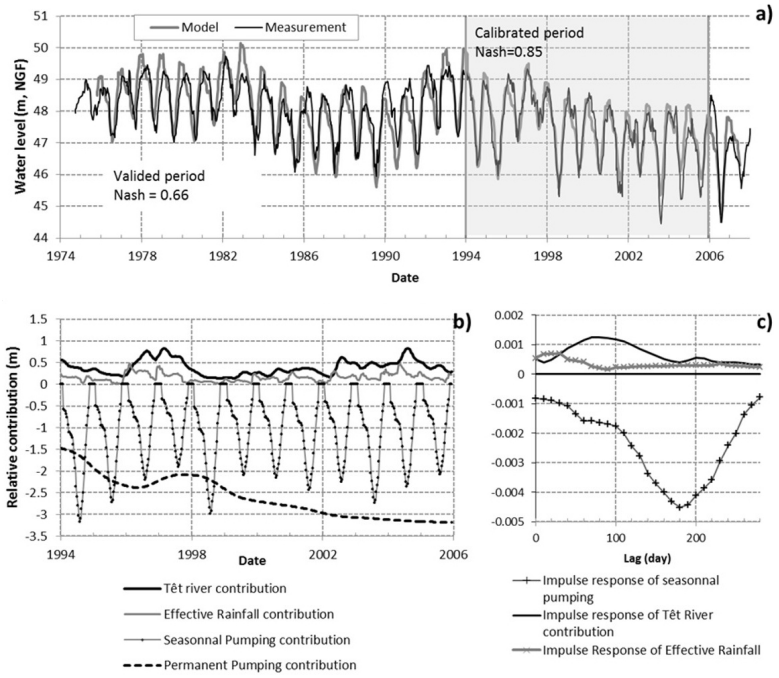

Figure 11. Inverse modeling of Pliocene confined aquifer (Perpignan Piezometer) with a 10 day step. The measured and simulated piezometry is shown **(a)** as well as the relative contributions of the recharge, pumping, and Têt river components **(b)** and their impulse responses **(c)**.

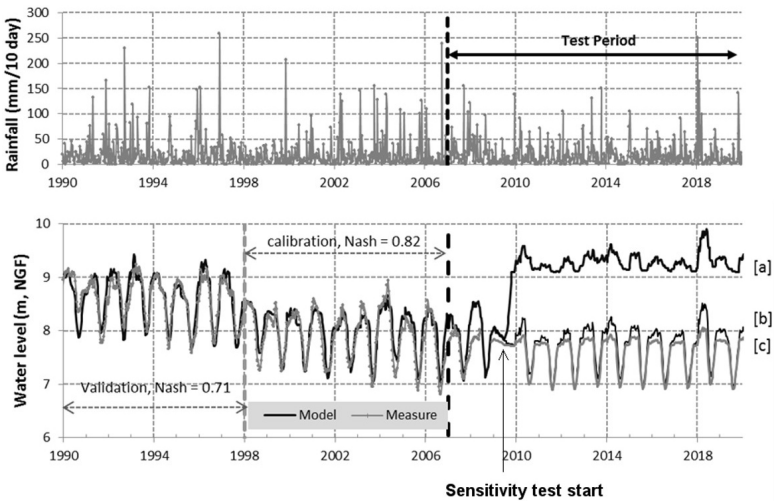

Figure 12. Sensitivity test of the model constructed for the Argelès piezometer for various conditions: variation of the piezometry calculated by the model in the absence of pumping [a] and for two precipitation situations, taking pumping into account: [b] = 50 % of the computed rain for the period 2008–2017 and [c] = 10 % of the computed rain for the period 2008–2017 (SP and PP pumping conditions identical to those of 2008).

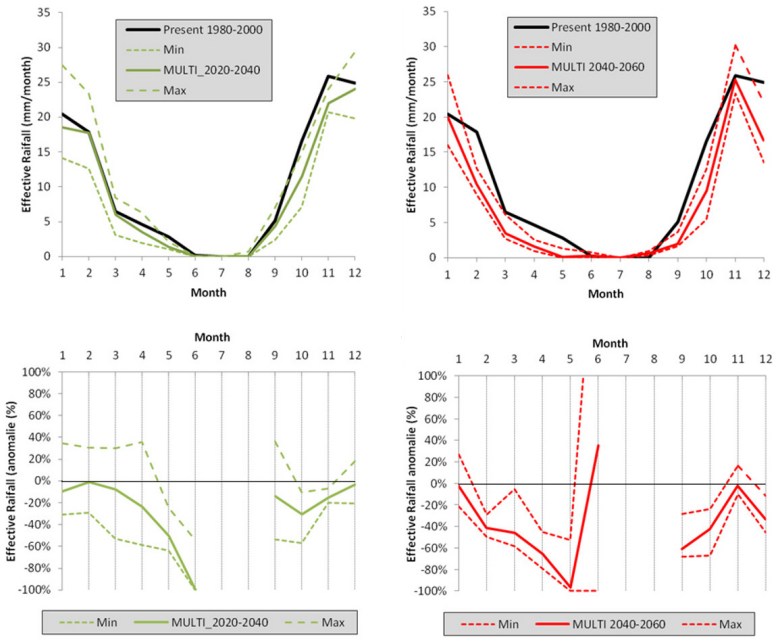

Figure 13. Variation of mean monthly values of effective rainfall for the reference period (1980–2000) and the short- (2020–2040) and medium- (2040–2060) term periods. The dashed lines represent the scenarios' dispersions limited by the minimum and maximum values of monthly averages considering all scenarios. January = Month 1 and December = Month 12.

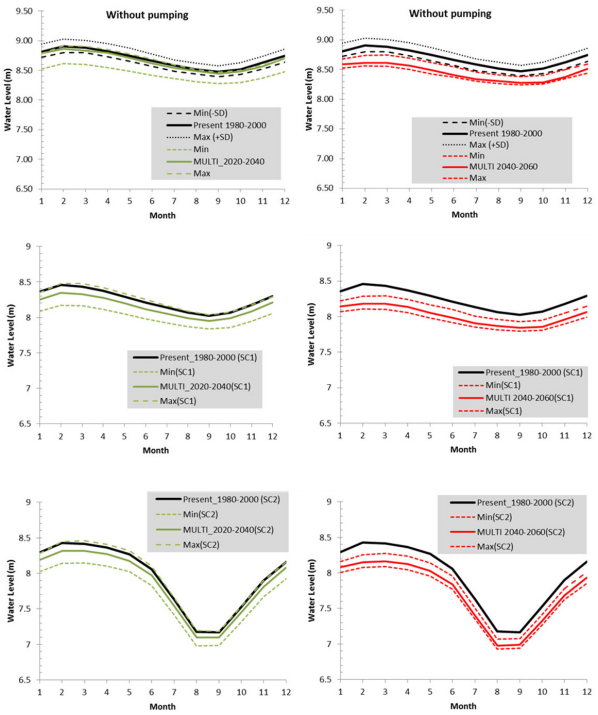

Figure 14. Variation of interannual monthly means of the piezometric levels simulated for the Argelès piezometer: reference period (1980–2000), short- (2020–2040) and medium- (2040–2060) term. The minimum and maximum envelope curves correspond to the extreme values across all scenarios. January = Month 1 and December = Month 12. Three different situations are simulated: (top) no pumping; (middle) with PP and without SP (SC1); and (bottom) with PP and SP (SC2).